Magnetic order on a frustrated spin-$\frac{1}{2}$ Heisenberg antiferromagnet on the Union Jack lattice

R. F. Bishop,[1] P. H. Y. Li,[1] D. J. J. Farnell,[2] and C. E. Campbell[3]
[1]*School of Physics and Astronomy, The University of Manchester, Schuster Building, Manchester M13 9PL, United Kingdom*
[2]*Health Methodology Research Group, School of Community-Based Medicine, The University of Manchester, Jean McFarlane Building, University Place M13 9PL, United Kingdom*
[3]*School of Physics and Astronomy, University of Minnesota, 116 Church Street SE, Minneapolis, Minnesota 55455, USA*
(Received 13 April 2010; revised manuscript received 22 June 2010; published 15 July 2010)

We use the coupled cluster method (CCM) to study the zero-temperature phase diagram of a two-dimensional frustrated spin-half antiferromagnet, the so-called Union Jack model. It is defined on a square lattice such that all nearest-neighbor pairs are connected by bonds with a strength $J_1>0$, but only half the next-nearest-neighbor pairs are connected by bonds with a strength $J_2 \equiv \kappa J_1 > 0$. The bonds are arranged such that on the 2×2 unit cell they form the pattern of the Union Jack flag. Alternating sites on the square lattice are thus four-connected and eight-connected. We find strong evidence for a first phase transition between a Néel antiferromagnetic phase and a canted ferrimagnetic phase at a critical coupling $\kappa_{c_1}=0.66\pm 0.02$. The transition is an interesting one, at which the energy and its first derivative seem continuous, thus providing a typical scenario of a second-order transition (just as in the classical case for the model), although a weakly first-order transition cannot be excluded. By contrast, the average on-site magnetization approaches a nonzero value $M_{c_1}=0.195\pm 0.005$ on both sides of the transition, which is more typical of a first-order transition. The slope, $dM/d\kappa$, of the order parameter curve as a function of the coupling strength κ, also appears to be continuous, or very nearly so, at the critical point κ_{c_1}, thereby providing further evidence of the subtle nature of the transition between the Néel and canted phases. Our CCM calculations provide strong evidence that the canted ferrimagnetic phase becomes unstable at large values of κ, and hence we have also used the CCM with a model collinear semistripe-ordered ferrimagnetic state in which alternating rows (and columns) are ferromagnetically and antiferromagnetically ordered, and in which the spins connected by J_2 bonds are antiparallel to one another. We find tentative evidence, based on the relative energies of the two states, for a second zero-temperature phase transition between the canted and semistripe-ordered ferrimagnetic states at a large value of the coupling parameter around $\kappa_{c_2}\approx 125\pm 5$. This prediction, however, is based on an extrapolation of the CCM results for the canted state into regimes where the solutions have already become unstable and the CCM equations based on the canted state at any level of approximation beyond the lowest have no solutions. Our prediction for κ_{c_2} is hence less reliable than that for κ_{c_1}. Nevertheless, if this second transition at κ_{c_2} does exist, our results clearly indicate it to be of first-order type.

DOI: 10.1103/PhysRevB.82.024416 PACS number(s): 75.10.Jm, 75.30.Gw, 75.40.−s, 75.50.Ee

I. INTRODUCTION

Quantum magnetism at zero temperature for lattices in two spatial dimensions[1–3] is an important and fascinating subject because such systems display a wide variety of behavior, including semiclassical Néel ordering, two-dimensional (2D) quantum "spirals," valence-bond crystals/solids, and spin liquids. The behavior of these systems is driven by the nature of the underlying crystallographic lattice, the number and range of bonds on this lattice, and the spin quantum numbers of the atoms localized to the sites on the lattice. There are very few exact results for quantum spin systems on 2D lattices, and so the application of approximate methods is crucial to their understanding. The theoretical investigation of these models has been strongly mirrored by the discovery and experimental investigation of new quasi-2D magnetic materials. It seems clear that we can only form a complete picture of such 2D quantum spin-lattice systems by considering a wide range of possible scenarios that are often inspired (or followed shortly afterwards) by experimental studies.

A prototypical case is presented by the spin-half square-lattice Heisenberg antiferromagnet (HAF) model. This model has been studied extensively via a range of approximate techniques.[3–6] Its basic properties have been well established, where, for example, approximate results for the order parameter indicate that about 61% of the classical Néel ordering persists in the quantum limit at zero temperature. A review of the properties of the spin-half square-lattice HAF is given in Ref. 7. The most accurate results for this model are provided by quantum Monte Carlo (QMC) simulations.[4] Indeed, QMC techniques generally provide the benchmark for quantum magnets in two spatial dimensions. However, its use is severely limited by the "sign problem," which is often a consequence of quantum frustration in the context of lattice spin systems.

A common theme has also begun to emerge recently when frustrating next-nearest-neighbor (NNN) bonds with strength $J_2>0$ are added to the basic spin-half square-lattice HAF with nearest-neighbor (NN) bonds with strength $J_1>0$. The frustrating J_2 bonds may be added on some or all of the square plaquettes of the lattice and/or across both or only one of the diagonals of each plaquette. Perhaps the prototypical such model is the so-called spin-half J_1-J_2 model in which all possible NNN bonds are included. Recent interest in this model has been reinvigorated by the discovery of various

layered magnetic materials, such as Li_2VOSiO_4, Li_2VOGeO_4, $VOMoO_4$, and $BaCdVO(PO_4)_2$. Several approximate methods have been used to simulate the properties of this system including the coupled cluster method (CCM),[8–12] series expansion (SE) techniques,[13–17] exact diagonalization (ED) methods,[18–20] and hierarchical mean-field calculations.[21] These approximate techniques have established conclusively that there are two phases exhibiting magnetic long-range order (LRO) at small and at large values of $\kappa \equiv J_2/J_1$, respectively. For $\kappa < \kappa_{c_1} \approx 0.4$ the ground-state (gs) phase exhibits (NN) Néel magnetic LRO, whereas for $\kappa > \kappa_{c_2} \approx 0.6$ it exhibits collinear striped LRO in which alternating rows (or columns) of the square lattice have opposite spins, with the spins on each row (or columns) aligned, so that the Néel order is between NNN pairs. The intermediate region consists of a quantum paramagnetic state without magnetic LRO.

Several other models in this general class of spin-half models with both NN and NNN interactions have prompted recent interest. They all involve the removal of some of the NNN J_2 bonds from the fundamental J_1-J_2 model. One such example is the Shastry-Sutherland model,[22–24] realized experimentally by the magnetic material $SrCu(BO_3)_2$, which involves the removal of three-quarters of the J_2 bonds. Whereas the J_1-J_2 model on the 2D square lattice has each of the sites connected by eight bonds (four NN J_1 bonds and four NNN J_2 bonds) to other sites, the Shastry-Sutherland model has each of the sites connected by five bonds (four NN J_1 bonds and one NNN J_2 bond). A second example is the HAF on the anisotropic triangular lattice model (also known as the interpolating square-triangle model),[25] realized experimentally by the magnetic material Cs_2CuCl_4, which involves the removal of half the J_2 bonds from the original J_1-J_2 model. In this model each of the sites on the 2D square lattice is connected by six bonds (four NN J_1 bonds and two NNN J_2 bonds) to other sites, such that the remaining J_2 bonds connect equivalent NNN sites in each square plaquette. Although all of the models mentioned above show antiferromagnetic Néel ordering for small J_2, their phase diagrams for larger J_2 display a wide variety of behavior, including two-dimensional quantum spirals, valence-bond crystals/solids, and spin liquids. Thus, in the absence of any definitive theoretical argument, the best way to understand this class of NN/NNN models on the square lattice is to treat each one on a case-by-case basis.

In this paper we study another frustrated spin-half model that has both NN (J_1) and NNN (J_2) bonds on the square lattice, where these bonds form a pattern that resembles the "Union Jack" flag. Just as for the anisotropic triangular HAF described above, the Union Jack model on the 2D square lattice also has only one frustrating NNN bond per square plaquette, but these J_2 bonds are now arranged such that half the sites are connected by eight bonds (four NN J_1 bonds and four NNN J_2 bonds) to other sites while the other half are connected only by four J_1 bonds to their NN sites, as described more fully below in Sec. II. This model has previously been studied using spin-wave theory (SWT) (Refs. 26 and 27) and SE techniques.[28] As in the case of the spin-half interpolating square-triangle model, it was shown[26–28] that NN Néel order for the Union Jack model persists until a critical value of the frustrating NNN (J_2) bonds. However, in contrast to the interpolating square-triangle model, there exists a ferrimagnetic ground state in which spins on the eight-connected sites cant at a nonzero angle with respect to their directions in the corresponding Néel state. This model thus exhibits an overall magnetic moment in this regime, which is quite unusual for spin-half 2D materials with only Heisenberg bonds and which therefore preserve (spin-) rotational symmetries in the Hamiltonian. This model also presents us with a difficult computational task in order to simulate its properties. Here we wish to study this model using the CCM, which has consistently been shown to yield insight into a wide range of problems in quantum magnetism, and which we now hope will hence shed yet more light on the whole class of NN/NNN models as mentioned before. The dual associated features of a model with two sorts of sites with differing connectivities, and its consequent ferrimagnetic phase, are just those that are attracting the interest of the community now.

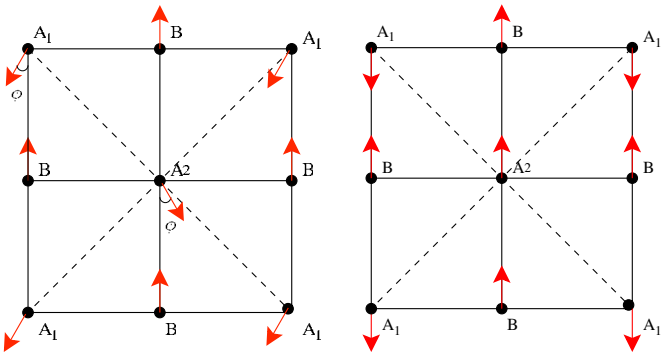

FIG. 1. (Color online) Union Jack model; — J_1; - - - J_2. (a) Canted state; (b) semistriped state. The unit cell is a square of side length 2.

II. MODEL

In this paper we now apply the CCM to the spin-half Union Jack model that has been studied recently by other means.[26–28] Its Hamiltonian is written as

$$H = J_1 \sum_{\langle i,j \rangle} \mathbf{s}_i \cdot \mathbf{s}_j + J_2 \sum_{[i,k]} \mathbf{s}_i \cdot \mathbf{s}_k, \tag{1}$$

where the operators $\mathbf{s}_i \equiv (s_i^x, s_i^y, s_i^z)$ are the quantum spin operators on lattice site i with $\mathbf{s}_i^2 = s(s+1)$ and $s = 1/2$. On the square lattice the sum over $\langle i,j \rangle$ runs over all distinct NN bonds with strength J_1 while the sum over $[i,k]$ runs over only half of the distinct NNN diagonal bonds having strength J_2 and with only one diagonal bond on each square plaquette as arranged in the pattern shown explicitly in Fig. 1. The unit cell is thus the 2×2 square shown in Fig. 1(a). (We note that, by contrast, the J_1-J_2 model discussed above, includes all of the diagonal NNN bonds on the square lattice.) We consider here the case where both sorts of bonds are antiferromagnetic, $J_1 > 0$ and $J_2 \equiv \kappa J_1 > 0$, and are hence acting to compete against (or to frustrate) each other. Henceforth we set $J_1 \equiv 1$. We consider the model equivalently defined by the

Union Jack geometry in which there are two sorts of sites, namely, the A sites with eight NN sites and the B sites with four NN sites, as shown in Fig. 1(a).

Considered classically rather than quantum mechanically, (and thus corresponding to the quantum case in the limit where the spin quantum number $s \to \infty$), the Union Jack model has only two gs phases as the parameter κ is varied over the range $(0, \infty)$. A simple variational analysis for the classical model reveals that for $0 < \kappa < 1/2$ the gs phase is Néel ordered, exactly as for the full J_1-J_2 model. Thus the Néel ordering induced by the J_1 bonds acting alone is preserved as the strength of the competing J_2 bonds is increased, until the critical value $\kappa_c^{\rm cl}=0.5$ is reached. For $\kappa > \kappa_c^{\rm cl}$ a new phase of lower energy emerges, just as in the full J_1-J_2 model. However, whereas for the full J_1-J_2 model that new phase is a classical striped state in which alternate rows (or columns) of spins are arranged antiparallel to one another, the new classical gs phase for the Union Jack model is the canted ferrimagnetic state shown in Fig. 1(a) in which the spins on each of the alternating A_1 and A_2 sites of the A sublattice are canted, respectively, at angles $(\pi \mp \phi)$ with respect to those on the B sublattice, all of the latter of which point in the same direction. On the A sublattice each site A_1 has four NN sites A_2, and vice versa. The angle between the NN spins on the A sublattice is thus 2ϕ.

The classical energy of the above canted state is thus

$$E = Ns^2(\kappa \cos 2\phi - 2 \cos \phi), \tag{2}$$

where $J_1 \equiv 1$ and $N \to \infty$ is the number of sites. Clearly the energy is extremized when

$$\sin \phi(1 - 2\kappa \cos \phi) = 0. \tag{3}$$

When $\kappa < \kappa_c^{\rm cl} \equiv 0.5$, the lowest energy corresponds to $\sin \phi = 0$ and hence to the Néel state. By contrast, when $\kappa > \kappa_c^{\rm cl} \equiv 0.5$ the lowest energy solution is the canted state with

$$\phi_{\rm cl} = \cos^{-1}\left(\frac{1}{2\kappa}\right). \tag{4}$$

Thus the classical gs energy is given by

$$E^{\rm cl} = \begin{cases} Ns^2(\kappa - 2) & \kappa < \kappa_c^{\rm cl} \equiv 0.5 \\ Ns^2\left(-\dfrac{1}{2\kappa} - \kappa\right) & \kappa > \kappa_c^{\rm cl} \equiv 0.5. \end{cases} \tag{5}$$

The classical phase transition at $\kappa = \kappa_c^{\rm cl} \equiv 0.5$ is of continuous (second-order) type with the gs energy and its first derivative both continuous functions of κ, although there are finite discontinuities in the second- and higher-order derivatives at $\kappa = \kappa_c^{\rm cl}$.

In the classical canted phase the total magnetization per site is $m^{\rm cl} = \frac{1}{2}s[1-(2\kappa)^{-1}]$, and the model thus exhibits ferrimagnetism in this phase. Whereas ferrimagnetism more commonly occurs when the individual ionic spins have different magnitudes on different sublattices, it arises here in a case where when the spins all have the same magnitude and all the interactions are antiferromagnetic in nature, but the frustration between them acts to produce an overall magnetization. The total magnetization m vanishes linearly as $\kappa \to \kappa_c^{\rm cl}$ from the canted phase and then remains zero in the Néel phase for $\kappa < \kappa_c^{\rm cl}$. The spontaneous breaking of the spin-rotation symmetry is also reflected by the vanishing of the energy gap on both sides of the transition. Clearly on both sides of the transition the translation symmetry of the lattice is also broken.

One of the aims of the present paper is to give a fully microscopic analysis of the Union Jack model for the quantum case where the spins all have spin quantum number $s = 1/2$. We are interested to map out the zero-temperature $(T=0)$ phase diagram of the model, including the positions and orders of any quantum phase transitions that emerge. In particular, we investigate the quantum analogs of the classical Néel and canted phases and calculate the effect of quantum fluctuations on the position and nature of the transition between them. We also aim to investigate, for particular regions of the control parameter κ, whether the quantum fluctuations may favor other phases, which have no classical counterparts. One such possible candidate is discussed below.

In the limit of $\kappa \to \infty$ the above classical limit corresponds to a canting angle $\phi \to \frac{1}{2}\pi$, such that the spins on the A sublattice become Néel ordered, as is expected. The spins on the antiferromagnetically ordered A sublattice are orientated at 90° to those on the ferromagnetically ordered B sublattice in this limit. In reality, of course, there is complete degeneracy at the classical level in this limit between all states for which the relative ordering directions for spins on A and B sublattices are arbitrary. Clearly the exact spin-$\frac{1}{2}$ limit should also comprise decoupled antiferromagnetic and ferromagnetic sublattices. However, one might now expect that this degeneracy in the relative spin orientations between the two sublattices is lifted by quantum fluctuations by the well-known phenomenon of *order by disorder*.[29] Just such a phase is known to exist in the full spin-$\frac{1}{2}$ J_1-J_2 model for values of $J_2/J_1 \gtrsim 0.6$, where it is the so-called collinear striped phase in which, on the square lattice, spins along (say) the rows in Fig. 1 order ferromagnetically while spins along the columns and diagonals order antiferromagnetically. We have also shown how such a striped state is stabilized by quantum fluctuations for values of $J_2'/J_1 \gtrsim 1.8$ for the spin-$\frac{1}{2}$ J_1-J_2' model defined on an anisotropic 2D lattice,[25] as discussed in Sec. I above.

The existence of the striped state as a stable phase for large values of the frustration parameter for both the spin-$\frac{1}{2}$ J_1-J_2 and J_1-J_2' models above is a reflection of the well-known fact that quantum fluctuations favor collinear ordering. In both cases the order-by-disorder mechanism favors the collinear state from the otherwise infinitely degenerate set of available states at the classical level. For the present Union Jack model the corresponding collinear state that might perhaps be favored by the order-by-disorder mechanism is the so-called semistriped state shown in Fig. 1(b) where the A sublattice is now Néel ordered in the same direction as the B sublattice is ferromagnetically ordered. Alternate rows (or columns) are thus ferromagnetically and antiferromagnetically ordered in the same direction. We investigate the possibility below that such a semistripe-ordered phase may be stabilized by quantum fluctuations at larger values of κ.

III. COUPLED CLUSTER METHOD

The CCM (see, e.g., Refs. 30–32 and references cited therein) that we employ here is one of the most powerful and most versatile modern techniques available to us in quantum many-body theory. It has been applied very successfully to various quantum magnets (see Refs. 8–12, 23–25, and 32–36 and references cited therein). The method is particularly appropriate for studying frustrated systems, for which some of the main alternative methods either cannot be applied or are sometimes only of limited usefulness, as explained below. For example, QMC techniques are particularly plagued by the sign problem for such systems, and the ED method is restricted in practice by available computational power, particularly for $s>1/2$, to such small lattices that it is often insensitive to the details of any subtle phase order present.

The method of applying the CCM to quantum magnets has been described in detail elsewhere (see, e.g., Refs. 30–35 and references cited therein). It relies on building multispin correlations on top of a chosen gs model state $|\Phi\rangle$ in a systematic hierarchy of LSUBn approximations (described below) for the correlation operators S and $\tilde{S}$ that parametrize the exact gs ket and bra wave functions of the system, respectively, as $|\Psi\rangle=e^{S}|\Phi\rangle$ and $\langle\tilde{\Psi}|=\langle\Phi|\tilde{S}e^{-S}$. In the present case we use three different choices for the model state $|\Phi\rangle$, namely, either of the classical Néel and canted states, as well as the semistriped state. Note that for the canted phase we perform calculations for arbitrary canting angle ϕ [as shown in Fig. 1(a)], and then minimize the corresponding LSUBn approximation for the energy with respect to ϕ, $E_{\mathrm{LSUB}n}(\phi)\rightarrow\min\Leftrightarrow\phi=\phi_{\mathrm{LSUB}n}$. Generally (for $n>2$) the minimization must be carried out computationally in an iterative procedure, and for the highest values of n that we use here the use of supercomputing resources was essential. Results for the canting angle $\phi_{\mathrm{LSUB}n}$ will be given later. We choose local spin coordinates on each site in each case so that all spins in $|\Phi\rangle$, whatever the choice, point in the negative z direction (i.e., downward) by definition in these local coordinates.

Then, in the LSUBn approximation all possible multispin-flip correlations over different locales on the lattice defined by n or fewer contiguous lattice sites are retained. The numbers of such distinct (i.e., under the symmetries of the lattice and the model state) fundamental configurations of the current model in various LSUBn approximations are shown in Table I. We note that the distinct configurations given in Table I are defined with respect to the Union Jack geometry described in Sec. II, in which the B sublattice sites of Fig. 1(a) are defined to have four NN sites and the A sublattice sites are defined to have the eight NN sites joined to them either by J_1 or J_2 bonds. If we chose instead to work in the square-lattice geometry every site would have four NN sites. The coupled sets of equations for these corresponding numbers of coefficients in the operators S and $\tilde{S}$ are derived using computer algebra[37] and then solved[37] using parallel computing. We note that such CCM calculations using up to about 10^5 fundamental configurations or so have been previously carried out many times using the CCCM code[37] and heavy parallelization. A significant extra computational burden arises here for the canted state due to the need to optimize the quantum canting angle ϕ at each LSUBn level of approximation as described above. Furthermore, for many model states the quantum number $s_T^z\equiv\Sigma_{i=1}^{N}s_i^z$ in the original global spin-coordinate frame, may be used to restrict the numbers of fundamental multispin-flip configurations to those clusters that preserve s_T^z as a good quantum number. This is true for the Néel state where $s_T^z=0$ and for the semistriped state for which $s_T^z=N/4$, where N is the number of lattice sites. However, for the canted model state that symmetry is absent, which largely explains the significantly greater number of fundamental configurations shown in Table I for the canted state at a given LSUBn order. Hence, the maximum LSUBn level that we can reach here for the canted state, even with massive parallelization and the use of supercomputing resources, is LSUB7. For example, to obtain a single data point for a given value of κ (i.e., for a given value of J_2, with $J_1=1$) for the canted phase at the LSUB7 level typically required about 0.3 h computing time using 600 processors simultaneously. However, for values of κ near to termination points at which CCM solutions using that model state disappear (as described more fully below), the computing time typically increased significantly.

TABLE I. Number of fundamental LSUBn configurations (N_f) for semistriped and canted states of the spin-$\frac{1}{2}$ Union Jack model, based on the Union Jack geometry defined in the text.

	N_f	
Method	Semistriped	Canted
LSUB2	3	5
LSUB3	5	42
LSUB4	41	199
LSUB5	194	1259
LSUB6	1159	8047
LSUB7	6862	56442

At each level of approximation we may then calculate a corresponding estimate of the gs expectation value of any physical observable such as the energy E and the magnetic order parameter, $M\equiv-\frac{1}{N}\Sigma_{i=1}^{N}\langle\tilde{\Psi}|s_i^z|\Psi\rangle$, defined in the local, rotated spin axes, and which thus represents the average on-site magnetization. Note that M is just the usual sublattice (or staggered) magnetization per site for the case of the Néel state as the CCM model state, for example.

It is important to note that we never need to perform any finite-size scaling, since all CCM approximations are automatically performed from the outset in the infinite-lattice limit, $N\rightarrow\infty$, where N is the number of lattice sites. However, we do need as a last step to extrapolate to the $n\rightarrow\infty$ limit in the LSUBn truncation index n. We use here the well-tested[33,34] empirical scaling laws

$$E/N=a_0+a_1n^{-2}+a_2n^{-4}, \tag{6}$$

$$M=b_0+b_1n^{-1}+b_2n^{-2}. \tag{7}$$

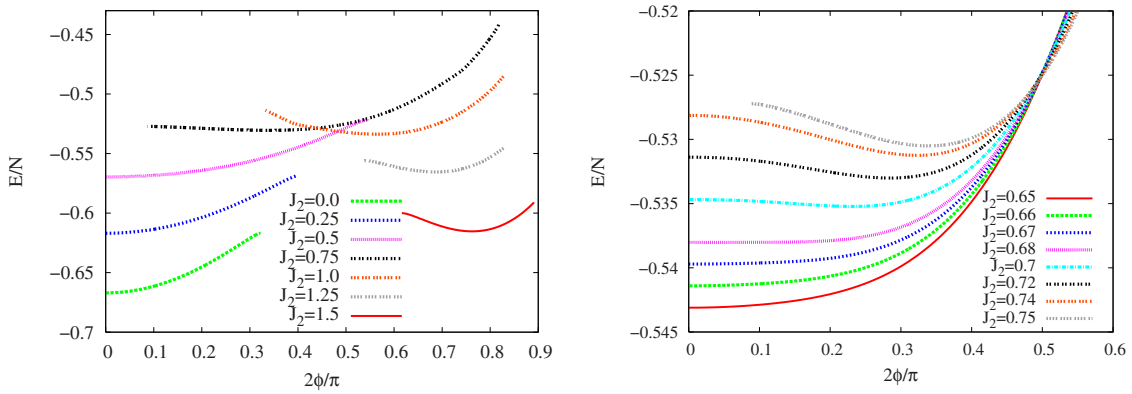

FIG. 2. (Color online) Ground-state energy per spin of the spin-$\frac{1}{2}$ Union Jack Hamiltonian of Eq. (1) with $J_1 \equiv 1$, using the LSUB6 approximation of the CCM with the canted model state, versus the canting angle ϕ, for some illustrative values of J_2 in the range $0 \leq J_2 \leq 1.5$ for Fig. 2(a) and $0.65 \leq J_2 \leq 0.75$ for Fig. 2(b). For $J_2 \lesssim 0.68$ in this approximation the minimum is at $\phi = 0$ (Néel order) whereas for $J_2 \gtrsim 0.68$ the minimum occurs at $\phi = \phi_{\text{LSUB6}} \neq 0$, indicating a phase transition at $J_2 \approx 0.68$ in this LSUB6 approximation.

IV. RESULTS

We report here on CCM calculations for the present spin-$\frac{1}{2}$ Union Jack model Hamiltonian of Eq. (1) for given parameters $(J_1 = 1, J_2)$, based, respectively, on the Néel, canted, and semistriped states as CCM model states. Our computational power is such that we can perform LSUBn calculations for each model state with $n \leq 7$. We note that, as has been well documented in the past,[38] the LSUBn data for both the gs energy per spin E/N and the average on-site magnetization M converge differently for the even-n and the odd-n sequences, similar to what is frequently observed in perturbation theory.[39] Since, as a general rule, it is desirable to have at least $(n+1)$ data points to fit to any fitting formula that contains n unknown parameters, we prefer to have at least four results for different values of the LSUBn truncation index n to fit to Eqs. (6) and (7). However, for all of our extrapolated results below we perform separate extrapolations using even and odd LSUBn sequences with $n = \{2,4,6\}$ and $n = \{3,5,7\}$.

A. Néel state versus the canted state

We report first on results obtained using the Néel and canted model states. While classically we have a second-order phase transition from Néel order (for $\kappa < \kappa_c^{\text{cl}}$) to canted order (for $\kappa > \kappa_c^{\text{cl}}$), where $\kappa \equiv J_2/J_1$, at a value $\kappa_c^{\text{cl}} = 0.5$, using the CCM we find strong indications of a shift of this critical point to a higher value $\kappa_{c_1} \approx 0.66$ in the spin-$\frac{1}{2}$ quantum case as we explain in detail below. Thus, for example, curves such as those shown in Fig. 2 show that the Néel model state ($\phi = 0$) gives the minimum gs energy for all values of $\kappa < \kappa_{c_1}$, where $\kappa_{c_1} = \kappa_{c_1}^{\text{LSUB}n}$ is also dependent on the level of LSUBn approximation, as we see clearly in Fig. 3.

By contrast, for $\kappa > \kappa_{c_1}$ the minimum in the energy is found to occur at a value $\phi \neq 0$. If we consider the canting angle ϕ itself as an order parameter (i.e., $\phi = 0$ for Néel order and $\phi \neq 0$ for canted order) a typical scenario for a first-order phase transition would be the appearance of a two-minimum structure for the gs energy as a function of ϕ. If we therefore admit such a scenario, in the typical case one would expect

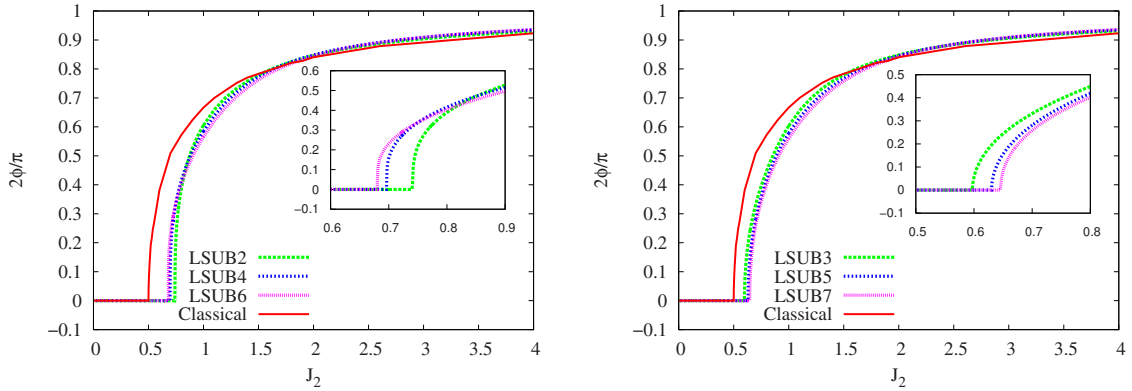

(a) $n = \{2, 4, 6\}$ (b) $n = \{3, 5, 7\}$

FIG. 3. (Color online) The angle $\phi_{\text{LSUB}n}$ that minimizes the energy $E_{\text{LSUB}n}(\phi)$ of the spin-$\frac{1}{2}$ Union Jack Hamiltonian of Eq. (1) with $J_1 \equiv 1$, in the LSUBn approximations with (a) $n = \{2,4,6\}$ and (b) $n = \{3,5,7\}$, using the canted model state, versus J_2. The corresponding classical result ϕ_{cl} from Eq. (4) is shown for comparison. We find in the LSUBn quantum case with $n > 2$ a weakly first-order phase transition or second-order phase transition (e.g., for LSUB6 at $J_2 \approx 0.680$ and LSUB7 at $J_2 \approx 0.646$). By contrast, in the classical case there is a second-order phase transition at $J_2 = 0.5$.

various special points in the transition region, namely, the phase transition point κ_{c_1} itself where the two minima have equal depth, plus one or two instability points κ_{i_1} and κ_{i_2} where one or other of the minima (at $\phi=0$ and $\phi\neq 0$, respectively) disappears. By contrast, a second-order phase transition might manifest itself via a one-minimum structure for the gs energy as a function of ϕ, in which the single minimum moves smoothly and continuously from the value $\phi=0$ for all values of $\kappa<\kappa_{c_1}$ to nonzero value $\phi\neq 0$ for $\kappa>\kappa_{c_1}$.

We show in Fig. 2 our results for the LSUB6 approximation based on the canted (or Néel) state as the CCM model state. Very similar curves occur for other LSUBn approximations. A close inspection of curves such as those shown in Fig. 2 for the LSUB6 case shows that what happens for this model at this level of approximation is that for $\kappa\lesssim 0.68$ the only minimum in the gs energy is at $\phi=0$ (Néel order). As this value is approached from below the LSUB6 energy curves become extremely flat near $\phi=0$, indicating the disappearance at $\phi=0$ of the second derivative $d^2E/d\phi^2$ (and possibly also of one or more of the higher derivatives $d^nE/d\phi^n$ with $n\geq 3$), as well as of the first derivative $dE/d\phi$. Then, for all values $\kappa\gtrsim 0.68$ the LSUB6 curves develop a minimum at a value $\phi\neq 0$ which is also the global minimum. The state for $\phi\neq 0$ is thus the quantum analog of the classical canted phase. The fact that the antiferromagnetic Néel order survives into the classically unstable regime is another example of the well-known phenomenon that quantum fluctuations tend to promote collinear order in magnetic spin-lattice systems, as has been observed in many other such cases (see, e.g., Refs. 34 and 40). Thus, this collinear Néel-ordered state survives into a region where classically it becomes unstable with respect to the noncollinear canted state.

A close inspection of the curves shown in Fig. 3 for various LSUBn approximation shows that the crossover from one minimum ($\phi=0$, Néel) solution to the other ($\phi\neq 0$, canted) appears to be continuous for the odd-n sequence, thus indicating a second-order transition according to the above scenario. By contrast, for the even-n sequence with $n>2$ the curves in Fig. 3 become very steep in the crossover region just above $\kappa_{c_1}^{\mathrm{LSUB}n}$ and due to the extremely flat nature of the gs energy curves as a function of ϕ in this region, as shown in Fig. 2, it is impossible to rule out a small but finite discontinuity in the curves of Fig. 2(a) for the even-n LSUBn sequence at $\kappa=\kappa_{c_1}^{\mathrm{LSUB}n}$. However, if the phase transition is, in fact, first order, it is certainly only very weakly so according to this criterion.

Thus, based on the evidence presented so far of the gs energies of the Néel and canted phases, it would appear that the transition at $\kappa=\kappa_{c_1}$ between these two phases is either second order, as in the classical phase, or weakly first order. Such a situation where the quantum fluctuations change the nature of a phase transition qualitatively from a classical second-order type to a quantum first-order type has also been seen previously in the comparable spin-$\frac{1}{2}$ HAF models that interpolate continuously between square and triangular lattices,[25] and between square and honeycomb lattices,[34] respectively. In the present spin-$\frac{1}{2}$ Union Jack model, however, the CCM gs energy results appear to favor a second-order transition, although the extreme insensitivity of the gs energy to the canting angle ϕ near the crossover region, especially for the even-n LSUBn sequence with $n>2$, means that we cannot rule out a weakly first-order transition. The evidence to date indicates, however, that the quantum phase transition at κ_{c_1} is a subtle one. Furthermore, the present spin-$\frac{1}{2}$ Union Jack model appears, on the evidence to date, to behave somewhat differently (viz., in some senses "more classically") than its corresponding spin-$\frac{1}{2}$ interpolating square-triangle Heisenberg antiferromagnet counterpart.[25] Further evidence from Fig. 3 appears to back up this observation. Thus, we see from Fig. 3 that the quantum canting angle ϕ approaches its asymptotic value $\pi/2$ as $\kappa\rightarrow\infty$ slightly faster than does the corresponding classical value. By contrast, in the case of the spin-$\frac{1}{2}$ interpolating square-triangle Heisenberg antiferromagnet,[25] the corresponding pitch angle ϕ of the spiral phase (that is the analog of the canted phase for the present model) approaches its similar asymptotic value $\pi/2$ as $\kappa\rightarrow\infty$ *very much* faster than does the classical value. We also discuss this difference more fully below, where we find further evidence that quantum fluctuations modify the classical behavior of the Union Jack model rather less than they do for its corresponding spin-$\frac{1}{2}$ interpolating square-triangle Heisenberg antiferromagnet counterpart.

TABLE II. The critical value $\kappa_{c_1}^{\mathrm{LSUB}n}$ at which the transition between the Néel phase ($\phi=0$) and the canted phase ($\phi\neq 0$) occurs in the LSUBn approximation using the CCM with (Néel or) canted state as model state.

Method	$\kappa_{c_1}^{\mathrm{LSUB}n}$
LSUB2	0.740
LSUB4	0.696
LSUB6	0.680
LSUB∞ [a]	0.651 ± 0.001.
LSUB∞ [b]	0.676 ± 0.004.
LSUB3	0.597
LSUB5	0.630
LSUB7	0.645
LSUB∞ [a]	0.681 ± 0.001.
LSUB∞ [b]	0.653 ± 0.004.

[a]Based on $\kappa_{c_1}^{\mathrm{LSUB}n}=a_0+a_1n^{-1}$, with $n=\{2,4,6\}$ or $n=\{3,5,7\}$.
[b]Based on $\kappa_{c_1}^{\mathrm{LSUB}n}=b_0+b_1n^{-2}$, with $n=\{2,4,6\}$ or $n=\{3,5,7\}$.

We show in Table II the critical values $\kappa_{c_1}^{\mathrm{LSUB}n}$ at which the transition between the Néel and canted phases occurs in the various LSUBn approximations shown in Fig. 3. In the past we have found that a simple linear extrapolation, $\kappa_{c_1}^{\mathrm{LSUB}n}=a_0+a_1n^{-1}$, yields a good fit to such critical points, as seems to be the case here too. The corresponding "LSUB∞" estimates from the LSUBn data in Table II are $\kappa_{c_1}=0.651\pm 0.001$ based on $n=\{2,4,6\}$ and $\kappa_{c_1}=0.681\pm 0.001$ based on $n=\{3,5,7\}$ where the quoted errors are simply the standard deviations from the two fits. Similar estimates based on an extrapolation $\kappa_{c_1}^{\mathrm{LSUB}n}=b_0+b_1n^{-2}$ are also shown in Table II, for which the standard deviations are clearly greater. The fact that the two estimates based on even-n and

odd-n LSUBn sequences differ slightly from one another is a reflection of the extreme insensitivity of the gs energy to the canting angle ϕ near $\kappa_{c_1}^{\mathrm{LSUB}n}$, and the difference between the two estimates is a rough indication of our real error bars on κ_{c_1}. We also present other independent estimates of κ_{c_1} below.

We note from Fig. 2 that for certain values of J_2 with $J_1 \equiv 1$ (or, equivalently, κ) CCM solutions at a given LSUBn level of approximation (viz., LSUB6 in Fig. 2) exist only for certain ranges of the canting angle ϕ. For example, for the pure square-lattice HAF ($\kappa=0$) the CCM LSUB6 solution based on a canted model state only exists for $0 \leq \phi \lesssim 0.161\pi$. In this case, where the Néel solution is the stable ground state, if we attempt to move too far away from Néel collinearity the CCM equations themselves become "unstable" and simply do not have a real solution. Similarly, we see from Fig. 2 that for $\kappa=1.5$ the CCM LSUB6 solution exists only for $0.308\pi \lesssim \phi \leq 0.445\pi$. In this case the stable ground state is a canted phase, and now if we attempt either to move too close to Néel collinearity or to increase the canting angle too close to its asymptotic value of $\pi/2$, the real solution terminates.

Such terminations of CCM solutions are very common and are very well documented.[32] In all such cases a termination point always arises due to the solution of the CCM equations becoming complex at this point, beyond which there exist two branches of entirely unphysical complex conjugate solutions.[32] In the region where the solution reflecting the true physical solution is real there actually also exists another (unstable) real solution. However, only the shown branch of these two solutions reflects the true (stable) physical ground state, whereas the other branch does not. The physical branch is usually easily identified in practice as the one which becomes exact in some known (e.g., perturbative) limit. This physical branch then meets the corresponding unphysical branch at some termination point (with infinite slope in Fig. 2) beyond which no real solutions exist. The LSUBn termination points are themselves also reflections of the quantum phase transitions in the real system and may be used to estimate the position of the phase boundary,[32] although we do not do so for this first critical point since we have more accurate criteria discussed above as well as below.

Before doing so, however, we wish to give some further indication of the accuracy of our results. Thus in Table III we show data for the case of the spin-$\frac{1}{2}$ HAF on the square lattice (corresponding to the case $\kappa=0$ of the present Union Jack model). We present our CCM results in various LSUBn approximations (with $2 \leq n \leq 7$) based on the Union Jack geometry using the Néel model state. Results are given for the gs energy per spin E/N, and the magnetic order parameter M. We also display our extrapolated ($n \to \infty$) results using the schemes of Eqs. (6) and (7) with the data sets $n=\{2,4,6\}$ and $n=\{3,5,7\}$. The results are clearly seen to be robust and consistent, and for comparison purposes we also show the corresponding results using a QMC technique[4] and from a linked-cluster series expansion (SE) method.[6] We note that for the square-lattice HAF no dynamic (or geometric) frustration exists and the Marshall-Peierls sign rule[41] applies and may be used to circumvent the QMC "minus-sign problem."

TABLE III. Ground-state energy per spin E/N and magnetic order parameter M (i.e., the average on-site magnetization) for the spin-$\frac{1}{2}$ square-lattice HAF. We show CCM results obtained for the Union Jack model with $J_1=1$ and $J_2=0$ using the Néel model state in various CCM LSUBn approximations defined on the Union Jack geometry described in Sec. II. We compare our extrapolated ($n \to \infty$) results using Eqs. (6) and (7) with the odd-n and even-n LSUBn data sets with other calculations.

Method	E/N	M
LSUB2	−0.64833	0.4207
LSUB3	−0.65044	0.4151
LSUB4	−0.66366	0.3821
LSUB5	−0.66398	0.3795
LSUB6	−0.66703	0.3630
LSUB7	−0.66724	0.3606
	Extrapolations	
LSUB∞ [a]	−0.6698	0.316
LSUB∞ [b]	−0.6704	0.304
QMC[c]	−0.669437(5)	0.3070(3)
SE[d]	−0.6693(1)	0.307(1)

[a]Based on $n=\{2,4,6\}$.
[b]Based on $n=\{3,5,7\}$.
[c]QMC (quantum Monte Carlo) for square lattice (Ref. 4).
[d]SE (series expansion) for square lattice (Ref. 6).

The QMC results[4] are thus extremely accurate for this limiting ($\kappa=0$) case only, and represent the best available results in this case. Our own extrapolated results are in good agreement with these QMC benchmark results, as found previously (see, e.g., Ref. 38 and references cited therein) for CCM calculations performed specifically using the square-lattice geometry, as well as for other CCM calculations for which the square-lattice HAF is a limit, such as for the spin-$\frac{1}{2}$ interpolating square-triangle J_1-J_2' model,[25] for which the triangular lattice geometry was employed. It is gratifying to note, in particular, that although the individual LSUBn results for the spin-$\frac{1}{2}$ square-lattice HAF depend on which geometry is used to define the configurations, the corresponding LSUB∞ extrapolations are in excellent agreement with one another.

In Fig. 4 we show the CCM results for the gs energy per spin in various LSUBn approximations based on the canted (and Néel) model states with the canting angle $\phi_{\mathrm{LSUB}n}$ chosen to minimize the energy $E_{\mathrm{LSUB}n}(\phi)$, as shown in Fig. 3. We also show separately the extrapolated (LSUB∞) results obtained from Eq. (6) using the separate data sets $n=\{2,4,6\}$ and $n=\{3,5,7\}$ as shown. As is expected from our previous discussion the energy curves themselves show very little evidence of the phase transition at $\kappa=\kappa_{c_1}$, with the energy and its first derivative seemingly continuous.

Much clearer evidence for the transition between the Néel and canted phases is observed in our corresponding results for the gs magnetic order parameter M (the average on-site magnetization) shown in Fig. 5. For the raw LSUBn data we display the results for the Néel phase only for values of $\kappa < \kappa_{c_1}^{\mathrm{LSUB}n}$ for clarity. However, the extrapolated (LSUB∞) re-

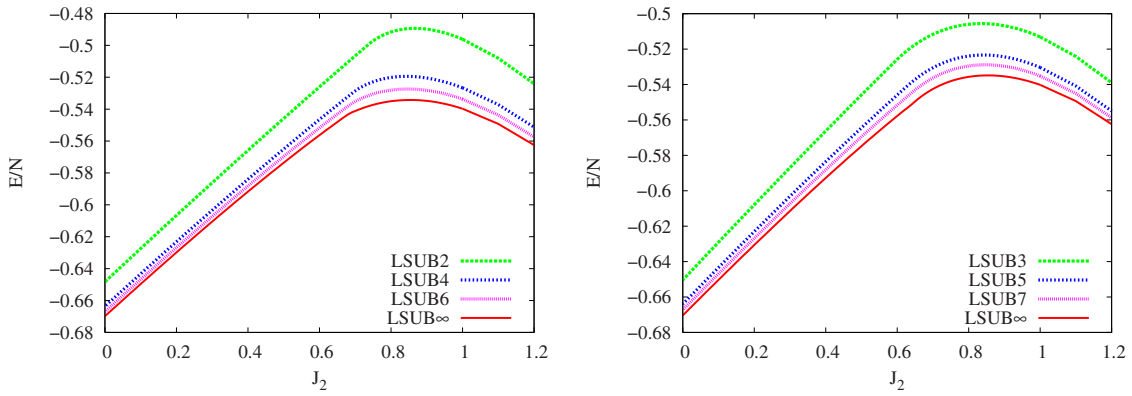

FIG. 4. (Color online) Ground-state energy per spin versus J_2 for the Néel and canted phases of the spin-$\frac{1}{2}$ Union Jack Hamiltonian of Eq. (1) with $J_1 \equiv 1$. The CCM results using the canted model state are shown for various LSUBn approximations with (a) $n=\{2,4,6\}$ and (b) $n=\{3,5,7\}$ with the canting angle $\phi=\phi_{\text{LSUB}n}$ that minimizes $E_{\text{LSUB}n}(\phi)$. We also show the $n\to\infty$ extrapolated result from using Eq. (6).

sults for the Néel phase are shown for all values of κ in the range shown and where $M>0$, using the extrapolation scheme of Eq. (7) and the LSUBn results based on the Néel model state. Once again we extrapolate odd-n and even-n LSUBn results separately. It is interesting to note from Fig. 5 that the raw LSUBn data show the transition at $\kappa_{c_1}^{\text{LSUB}n}$ more clearly for even values of n than for odd values of n. For the canted phase (for which $\phi_{\text{LSUB}n}\neq 0$) we can clearly only show the extrapolated (LSUB∞) results using Eq. (7), for regions of κ for which we have data for all of the set $n=\{2,4,6\}$ or $n=\{3,5,7\}$. We see from Table II that for the even-n values we are limited (by the LSUB2 results) to values $\kappa>\kappa_{c_1}^{\text{LSUB2}}\approx 0.740$ whereas for the odd-n values we are limited (by the LSUB7 results) to values $\kappa>\kappa_{c_1}^{\text{LSUB7}}\approx 0.645$. The separate odd-$n$ LSUB∞ extrapolation curves for M for the Néel and canted phases are seen from Fig. 5(b) to be extremely close at the value $\kappa=0.645$ and the curves appear to be about to meet at an angle which is either zero or very close to zero. A straightforward LSUB∞ extrapolation using Eq. (7) for the three whole LSUBn curves (Néel plus canted) with $n=\{3,5,7\}$ shows a value $\kappa_{c_1}\approx 0.637$ at which the extrapolated curve diverges (at zero or very small angle) from the corresponding LSUB∞ estimate for the Néel state shown in Fig. 5(b). For the corresponding even-n data shown in Fig. 5(a), simple extrapolations of the LSUB∞ curve to lower values of $\kappa<\kappa_{c_1}^{\text{LSUB2}}\approx 0.740$ using simple cubic or higher-order polynomial fits in κ give a corresponding estimate of $\kappa_{c_1}\approx 0.680$ at which the Néel and canted phases meet. Both even-n and odd-n LSUBn extrapolations yield a nonzero value for the average on-site magnetization of $M\approx 0.195\pm 0.005$ at the phase transition point κ_{c_1}. Thus the evidence from the behavior of the order parameter is that the transition at κ_{c_1} is a first-order one, in the sense that the order parameter does not go to zero at κ_{c_1}, although it is certainly continuous at this point, and with every indication that its derivative as a function of κ is also continuous (or very nearly so) at $\kappa=\kappa_{c_1}$.

We also show in Fig. 6 the corresponding extrapolated (LSUB∞) results for the average on-site magnetization as a function of J_2 (with $J_1\equiv 1$), or hence equivalently as a function of κ, for both the A sites (M_{A}) and the B sites (M_{B}) of the Union Jack lattice. We recall that, as shown in Fig. 1(a), each of the A and B sites is connected to four NN sites on the square lattice by J_1 bonds, whereas each of the A sites is

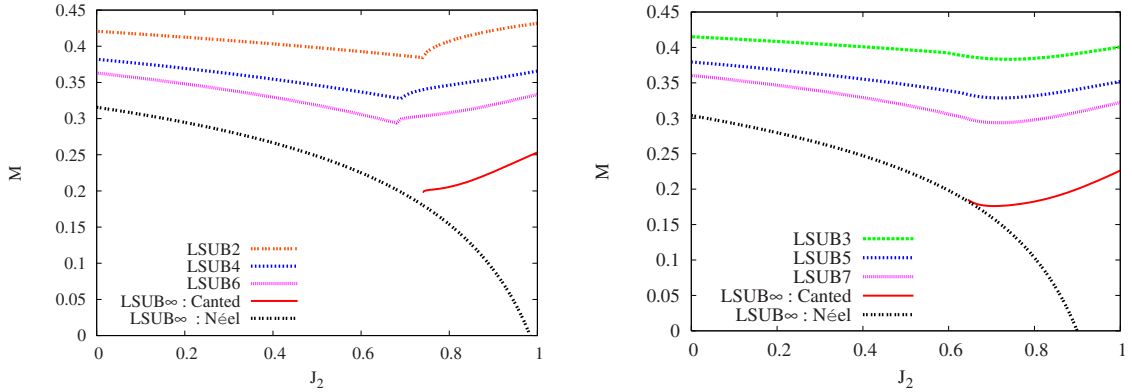

(a) $n=\{2,4,6\}$ (b) $n=\{3,5,7\}$

FIG. 5. (Color online) Ground-state magnetic order parameter (i.e., the average on-site magnetization) versus J_2 for the Néel and canted phases of the spin-$\frac{1}{2}$ Union Jack Hamiltonian of Eq. (1) with $J_1\equiv 1$. The CCM results using the canted model state are shown for various LSUBn approximations with (a) $n=\{2,4,6\}$ and (b) $n=\{3,5,7\}$ with the canting angle $\phi=\phi_{\text{LSUB}n}$ that minimizes $E_{\text{LSUB}n}(\phi)$. We also show the $n\to\infty$ extrapolated result from using Eq. (7).

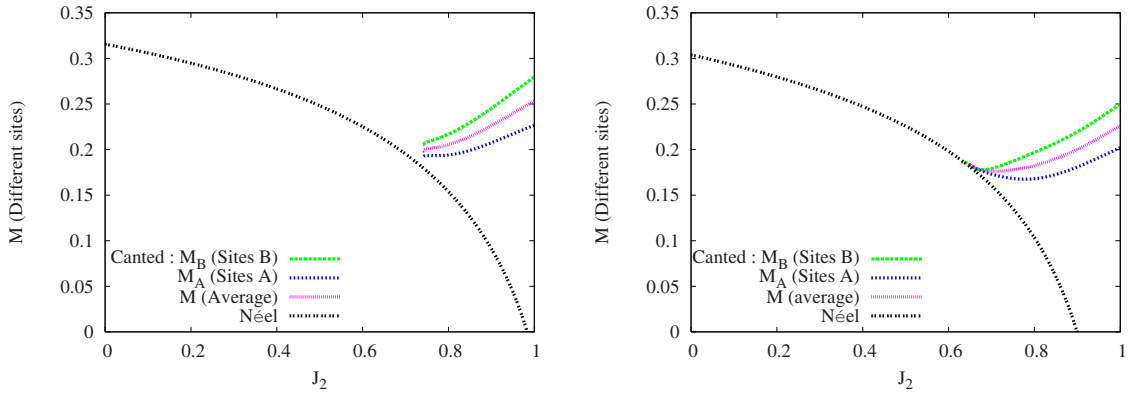

(a) $n = \{2, 4, 6\}$ (b) $n = \{3, 5, 7\}$

FIG. 6. (Color online) Extrapolated curves (LSUB∞) for the ground-state magnetic order parameters (i.e., the on-site magnetizations) M_A at sites A (joined by eight bonds to other sites) and M_B at sites B (joined by four bonds to other sites) of the Union Jack lattice [and see Fig. 1(a)] versus J_2 for the Néel and canted phases of the spin-$\frac{1}{2}$ Union Jack Hamiltonian of Eq. (1) with $J_1 \equiv 1$. The CCM results using the canted model state are shown for various LSUBn approximations ($n=\{2,4,6\}$ and $n=\{3,5,7\}$) with the canting angle $\phi=\phi_{\mathrm{LSUB}n}$ that minimizes $E_{\mathrm{LSUB}n}(\phi)$.

additionally connected to four NNN sites on the square lattice by J_2 bonds. The extrapolations are shown in exactly the same regions, and for the same reasons, as those shown in Fig. 5.

In Fig. 7 we also show the total gs magnetization per site, $m=\frac{1}{2}(M_B-M_A\cos\phi)$, from using our CCM LSUBn results with $n=\{2,4,6\}$ and with the canting angle $\phi=\phi_{\mathrm{LSUB}n}$ that minimizes $E_{\mathrm{LSUB}n}(\phi)$. Clearly $m=0$ in the Néel phase where $M_A=M_B$ and $\phi=0$. We also show in Fig. 7 the corresponding classical result $m^{\mathrm{cl}}=\frac{1}{2}s(1-\cos\phi_{\mathrm{cl}})=\frac{1}{4}[1-(2\kappa)^{-1}]$ in the canted phase (with $s=\frac{1}{2}$). A comparison of the extrapolated (LSUB∞) CCM curve with its classical counterpart shows very clearly that the quantum fluctuations for this spin-half Union Jack model modify the classical behavior only relatively modestly, providing further evidence to what we also noted earlier in relation to Fig. 3.

We also comment briefly on the large-J_2 behavior of our results for the canted phase. (We note that for computational purposes it is easier to rescale the original Hamiltonian of Eq. (1) by putting $J_2 \equiv 1$ and considering small values of J_1.) The most interesting feature of the CCM results using the canted state as model state is that in all LSUBn approximations with $n>2$ a termination point $\kappa_t^{\mathrm{LSUB}n}$ is reached, beyond which no real solution can be found, very similar to the termination points shown in Fig. 2. For the even-n sequence the values are $\kappa_t^{\mathrm{LSUB4}} \approx 80$ and $\kappa_t^{\mathrm{LSUB6}} \approx 80$, whereas for the odd-$n$ sequence the values are $\kappa_t^{\mathrm{LSUB3}} \approx 250$, $\kappa_t^{\mathrm{LSUB5}} \approx 85$, and $\kappa_t^{\mathrm{LSUB7}} \approx 55$. This is a first indication that the canted state becomes unstable at very large values of κ against the formation of another (as yet unknown) state, as we discuss further in Sec. IV B below.

Extrapolations of the gs energy using the data before the terminations points $\kappa_t^{\mathrm{LSUB}n}$ show that at large J_2 values we have $E/N \to -0.3349J_2$ using the even-n LSUBn series and $E/N \to -0.3352J_2$ using the odd-n series. These numerical coefficients are precisely half of the values quoted in Table III for the case $J_2=0$. This is exactly as expected since both the $\kappa \to 0$ and the $\kappa \to \infty$ limits of the Union Jack model are the square-lattice HAF, where in the latter case the square lattice contains only half the original sites, namely, the A sites. Similarly, the extrapolated LSUB∞ values at larger values of κ before the termination point for the on-site magnetization on the A sites are $M_A \to 0.317$ for the even-n LSUBn series and $M_A \to 0.306$ for the odd-n series. Both values are again remarkably consistent with those shown in Table III for the $J_2=0$ limit. The corresponding asymptotic values for the B-site magnetization are consistent with $M_B \to 0.5$, as expected for large values of J_2.

B. Canted state versus the semistriped state

We turn finally to our CCM results based on the use of the semistriped state shown in Fig. 1(b) as the model state. Unlike in the case of the corresponding use of the canted state as model state, the results based on the semistriped state do

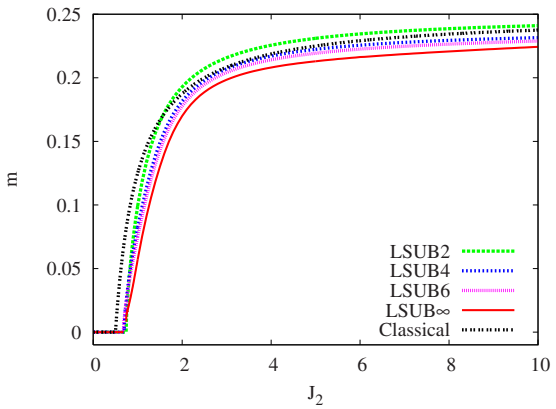

FIG. 7. (Color online) The total ground-state magnetization per site, $m=\frac{1}{2}(M_B-M_A\cos\phi)$, of the Union Jack lattice versus J_2 of the spin-$\frac{1}{2}$ Union Jack Hamiltonian of Eq. (1) with $J_1 \equiv 1$. The CCM results using the canted model state are shown for various LSUBn approximations ($n=\{2,4,6\}$) with the canting angle $\phi=\phi_{\mathrm{LSUB}n}$ that minimizes $E_{\mathrm{LSUB}n}(\phi)$. We also show the $n \to \infty$ extrapolated result from using Eq. (7) and compare it with the classical value $m^{\mathrm{cl}}=\frac{1}{4}(1-\cos\phi_{\mathrm{cl}})$.

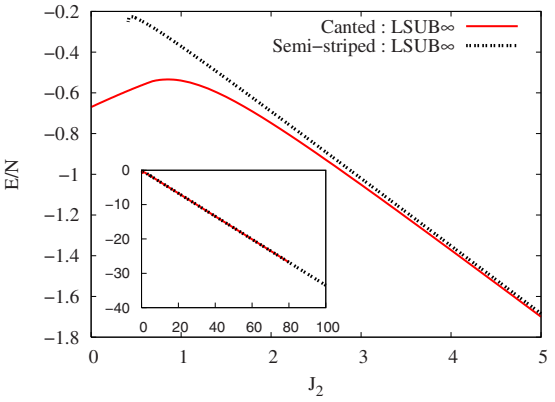

FIG. 8. (Color online) Comparison of the extrapolated (LSUB∞) curves for the ground-state energy per spin of the spin-$\frac{1}{2}$ Union Jack model, using the LSUBn data with $n=\{2,4,6\}$ fitted to Eq. (6), for the CCM based on canted and semistriped states as model states. The LSUB4 and the LSUB6 approximations (and hence also the extrapolated curve) for the canted model state terminate at $J_2 \approx 80$.

not terminate at a high value of J_2 (with $J_1 \equiv 1$). We found no indication of such a termination value at any LSUBn level of approximation for $2 \leq n \leq 7$ for values of $J_2 < 1000$. All indications are thus that the semistriped state is stable out to the $J_2 \to \infty$ limit. Indeed for these LSUBn levels the CCM solutions based on the semistriped state as model state exist for all values $J_2 > 1$. For example, the LSUB6 solution based on the semistriped state terminates at a lower end point $J_2 \approx 0.41$.

In Fig. 8 we compare the extrapolated (LSUB∞) values of the gs energy per spin, based in each case on the LSUBn results with $n=\{2,4,6\}$, for our CCM results using canted and semistriped states. Although results for the canted model state become unavailable for $J_2 \gtrsim 80$ for LSUB4 and LSUB6 approximations, the results based on the canted state lie lower in energy than those based on the semistriped state for all values of $J_2 \lesssim 80$ for which both sets of solutions exist. Although this is disappointing at first sight, the two sets of curves become extremely close for larger values of J_2 as can be seen from Fig. 8. Furthermore, we have also attempted a simple power-law extrapolation of the quantity $E/(NJ_2)$ for the gs energy of the canted state in powers of $1/J_2$, beyond the large-J_2 LSUBn termination points (viz., at $J_2 \approx 80$ for the LSUB6 approximation). Fits to sixth-, seventh-, and eighth-order polynomials give virtually identical results for values of J_2 in the range $80 \lesssim J_2 \lesssim 500$ and these extrapolated curves do indicate that there is a second phase transition at $\kappa_{c_2} \approx 125 \pm 5$ between canted and semistriped phases, such that for values $\kappa > \kappa_{c_2}$ the semistriped phase becomes lower in energy.

The gs energy in both canted and semistriped phases approaches the asymptotic value $E/N \approx -0.3349 J_2$ for large values of J_2 as $J_2 \to \infty$ (with $J_1 \equiv 1$). The corresponding asymptotic ($J_2 \to \infty$) values for the average on-site magnetization of the semistriped state are $M_A \to 0.317$ for the A sites and $M_B \to 0.5$ for the B sites.

V. DISCUSSION AND CONCLUSIONS

In this paper we have used the CCM to study the influence of quantum fluctuations on the zero-temperature gs phase diagram of a frustrated spin-half Heisenberg antiferromagnet (HAF) defined on the 2D Union Jack lattice. We have studied the case where the NN J_1 bonds are antiferromagnetic ($J_1 > 0$) and the competing NNN $J_2 \equiv \kappa J_1$ bonds in the Union Jack array have a strength in the range $0 \leq \kappa < \infty$. On the underlying bipartite square lattice there are thus two types of sites, viz., the A sites that are connected to the four NN sites on the B sublattice with J_1 bonds and to the four NNN on the A sublattice with J_2 bonds, and the B sites that are connected only to the four NN sites on the A sublattice with J_1 bonds. The $\kappa=0$ limit of the model thus corresponds to the spin-half HAF on the original square lattice (of A and B sites) while the $\kappa \to \infty$ limit corresponds to the spin-half HAF on the square lattice comprised of only A sites. We have seen that at the classical level (corresponding to the case where the spin quantum number $s \to \infty$) this Union Jack model has only two stable gs phases, one with Néel order for $\kappa < \kappa_c^{\rm cl} = 0.5$ and another with canted ferrimagnetic order for $\kappa > \kappa_c^{\rm cl}$. We have therefore first used these two classical states as CCM model states to investigate the effects of quantum fluctuations on them.

For the spin-half model we find that the phase transition between the Néel antiferromagnetic phase and the canted ferrimagnetic phase occurs at the higher value $\kappa_{c_1} = 0.66 \pm 0.02$. The evidence from our calculations is that the transition at κ_{c_1} is a subtle one. From the energies of the two phases it appears that the transition is either second order, as in the classical case, or possibly, weakly first order. However, on neither side of the transition at κ_{c_1} does the order parameter M (i.e., the average on-site magnetization) go to zero. Instead as $\kappa \to \kappa_{c_1}$ from either side, $M \to 0.195 \pm 0.005$, which is more indicative of a first-order transition. Furthermore, the slope $dM/d\kappa$ of the average on-site magnetization as a function of κ also seems to be either continuous or to have only a very weak discontinuity at $\kappa = \kappa_{c_1}$.

Before continuing with the possibility of a further phase we compare our results with those from previous calculations of the same model using spin-wave theory (SWT) (Refs. 26 and 27) and the linked-cluster SE method.[28] Collins *et al.*[26,27] used linear (or leading-order) spin-wave theory (LSWT) to show that on the basis of a comparison of the gs energies of the two phases, the phase transition between the Néel and canted phases is of first-order type and occurs at $\kappa_{c_1} \approx 0.84$. In LSWT the Néel staggered magnetization per site M remains substantial at this estimate of $\kappa_{c_1} \approx 0.84$. However, it is well known that LSWT results become unreliable near the transition region, and they surmised that the Néel order parameter M might vanish at or before this point, yielding a possible scenario where a second-order Néel transition might occur at a value $\kappa_{c_1} \lesssim 0.84$, followed by a possible intermediate spin-liquid phase (as in the pure J_1-J_2 model, as discussed in Sec. I), and then a first-order transition to the canted phase at a somewhat larger value of κ. Our own results provide no evidence at all for such an intermediate spin-liquid phase between the Néel antiferromagnetic and canted ferrimagnetic phases.

Although LSWT is known to give a reasonable description of the spin-$\frac{1}{2}$ Heisenberg antiferromagnet on the square lattice ($\kappa=0$), it is surely unable to model the frustrated or

intermediate regime accurately. Similar shortcomings of SWT have been noted by Igarashi[42] in the context of the related spin-$\frac{1}{2}$ J_1-J_2 model on the square lattice, discussed briefly in Sec. I. He showed that whereas its lowest-order version (LSWT) works well when $J_2=0$, it consistently overestimates the quantum fluctuations as the frustration J_2/J_1 increases. In particular he showed, by going to higher orders in SWT in powers of $1/s$, where s is the spin quantum number and LSWT is the leading order, that the expansion converges reasonably well for $J_2/J_1 \lesssim 0.35$, but for larger values of J_2/J_1, including the point $J_2/J_1=0.5$ of maximum classical frustration, the series loses stability. He also showed that the higher-order corrections to LSWT for $J_2/J_1 \lesssim 0.4$ make the Néel-ordered phase more stable than predicted by LSWT. He concluded that any predictions from SWT for the spin-$\frac{1}{2}$ J_1-J_2 model on the square lattice are likely to be unreliable for values $J_2/J_1 \gtrsim 0.4$. It is likely that a similar analysis of the SWT results for the spin-$\frac{1}{2}$ Union Jack model studied here would reveal similar shortcomings of LSWT as the frustration parameter $\kappa \equiv J_2/J_1$ is increased.

In a later paper by Zheng *et al.*,[28] SE techniques were applied to our spin-half Union Jack model and were compared with those from both LSWT for both the Néel and canted phases and modified second-order SWT for the Néel phase. Using the SE method for the Néel phase gave what these authors termed very clear evidence of a second-order phase transition at a critical coupling $\kappa_{c_1}=0.65\pm0.01$ at which the Néel staggered magnetization per site vanished. For higher couplings the system was seen to lie in the canted phase with no sign of any intermediate spin-liquid phase between these two magnetically ordered states. Use of the SE method in the canted phase produced a gs energy which continues smoothly from the Néel into the canted phase. Zheng *et al.*[28] found, furthermore, that in the canted phase the staggered magnetizations per site in both vertical and horizontal directions shown in Fig. 1(a) also appear to drop smoothly toward zero around the same value $\kappa_{c_1}=0.65\pm0.01$, albeit with very large error bars.

The above SE estimate for κ_{c_1} is clearly in excellent agreement with our own. However, whereas the evidence from the order parameter M from the SE technique clearly favors a second-order transition at κ_{c_1} at which $M\to0$ from both sides, our own CCM calculations clearly favor a first-order transition at which $M\to0.195\pm0.005$. We note, however, that the errors on the SE estimates for M become increasingly large as the phase transition at κ_{c_1} is approached from either side. We believe that this could easily account for the seeming discrepancy between our respective predictions for the order of the phase transition at κ_{c_1}. We note too that Zheng *et al.*[28] were themselves puzzled by the discrepancy between the prediction of SWT that the Néel magnetization per site M does not vanish at κ_{c_1} and that of the SE technique that M vanish does vanish there. While they recognized (as do we, as we discussed above) that SWT cannot be taken as an infallible guide, they found the huge difference with the prediction from the SE technique perturbing. Those authors ended by stating that, in their opinion, the nature of the transition from the Néel to the canted phase in the spin-half Union Jack model deserved further exploration. We believe that our own work reported here has considerably illuminated the transition at κ_{c_1}.

Neither SWT nor SE techniques have been applied to the possible semistriped state of Fig. 1(b) for the spin-half Union Jack model and so we have no results against which to compare our own. We were led to consider such a state as a possible gs phase of the model at large values of κ as discussed in Sec. II. Thus, to recapitulate, the $\kappa\to\infty$ limit of the canted phase of the Union Jack model (for either the quantum $s=1/2$ model considered here or the classical $s\to\infty$ case) gives a state in which the spins on the antiferromagnetically ordered A sublattice are orientated at 90° to those on the ferromagnetically ordered B sublattice. The actual $\kappa\to\infty$ limit should, in either case, be decoupled antiferromagnetic (A) and ferromagnetic (B) sublattices, with complete degeneracy at the classical level for all angles of relative ordering directions between the two sublattices. We argued that quantum fluctuations could, in principle, lift this degeneracy by the well-known order by disorder phenomenon.[29] Since quantum fluctuations are also well known from many spin-lattice problems to favor collinearity, there is a strong *a priori* possibility that the semistriped state of Fig. 1(b) might be energetically favored at large values of κ over the noncollinear state which is the $\kappa\to\infty$ limit of the canted state in which $\phi\to90°$.

Accordingly we repeated our CCM calculations using the semistriped state as model state. We found some evidence that at very large values of κ there might indeed be a second phase transition at $\kappa_{c_2}\approx125\pm5$, based on the relative energies of canted and semistriped states. Such a prediction is based, however, on an extrapolation of the data on the canted state into regimes where the CCM equations have no solution for LSUBn approximations with $n>3$, and hence cannot be regarded as being as reliable as our prediction for κ_{c_1}. If the phase transition at κ_{c_2} does exist it would be of first-order type according to our results. It would be of considerable interest to explore the possible transition at κ_{c_2} between canted and semistriped phases by other techniques, possibly including SWT and SE methods.

As has been noted elsewhere,[10] high-order CCM results of the sort presented here have been seen to provide accurate and reliable results for a wide range of such highly frustrated spin-lattice models. Many previous applications of the CCM to unfrustrated spin models have given excellent quantitative agreement with other numerical methods [including exact diagonalization (ED) of small lattices, quantum Monte Carlo (QMC), and SE techniques]. A typical example is the spin-half HAF on the square lattice, which is the $\kappa=0$ limit of the present model (and see Table III). It is interesting to compare for this $\kappa=0$ case, where comparison can be made with QMC results, the present CCM extrapolations of the LSUBn data for the infinite lattice to the $n\to\infty$ limit and the corresponding QMC or ED extrapolations for the results obtained for finite lattices containing N spins that have to be carried out to give the $N\to\infty$ limit. Thus, for the spin-$\frac{1}{2}$ HAF on the square lattice the "distance" between the CCM results for the ground-state energy per spin[38] at the LSUB6 (LSUB7) level and the extrapolated LSUB∞ value is approximately the same as the distance of the corresponding QMC result[43] for a

lattice of size $N=12\times12$ ($N=16\times16$) from its $N\to\infty$ limit. The corresponding comparison for the magnetic order parameter M is even more striking. Thus even the CCM LSUB6 result for M is closer to the LSUB∞ limit than any of the QMC results for M for lattices of N spins are to their $N\to\infty$ limit for all lattices up to size $N=16\times16$, the largest for which calculations were undertaken.[43] Such comparisons show, for example, that even though the distance between our LSUBn data points for M and the extrapolated ($n\to\infty$) LSUB∞ result shown in Fig. 5 may, at first sight, appear to be large, they are completely comparable to or smaller than those in alternative methods (where those other methods can be applied). Furthermore, where such alternative methods can be applied, as for the spin-$\frac{1}{2}$ HAF on the square lattice, the CCM results are in complete agreement with them.

By contrast, for frustrated spin-lattice models in two dimensions both the QMC and ED techniques face formidable difficulties. These arise in the former case due to the minus-sign problem present for frustrated systems when the nodal structure of the gs wave function is unknown, and in the latter case due to the practical restriction to relatively small lattices imposed by computational limits. The latter problem is exacerbated for incommensurate phases and is compounded due to the large (and essentially uncontrolled) variation of the results with respect to the different possible shapes of clusters of a given size.

For highly frustrated spin-lattice models like the present Union Jack model, a powerful numerical method, complementary to the CCM, is the linked-cluster SE technique.[13–17,44–48] The SE technique has also been applied to the present model.[28] Our own results have shed considerable light on the nature of the phase transition at κ_{c_1} observed by SE techniques and the discrepancies between the results from SE and SWT methods.

We end by remarking that it would also be of interest to repeat the present study for the case of the $s>1/2$ Union Jack model. The calculations for this case are more demanding due to an increase at a given LSUBn level of approximation in the number of fundamental configurations retained in the CCM correlation operators. Nevertheless, we hope to be able to report results for this system in the future.

ACKNOWLEDGMENTS

We thank the University of Minnesota Supercomputing Institute for Digital Simulation and Advanced Computation for the grant of supercomputing facilities, on which we relied heavily for the numerical calculations reported here. We are also grateful for the use of the high-performance computer service machine (i.e., the Horace clusters) of the Research Computing Services of the University of Machester.

[1] *Quantum Magnetism*, Lecture Notes in Physics Vol. 645, edited by U. Schollwöck, J. Richter, D. J. J. Farnell, and R. F. Bishop (Springer-Verlag, Berlin, 2004).
[2] G. Misguich and C. Lhuillier, in *Frustrated Spin Systems*, edited by H. T. Diep (World Scientific, Singapore, 2005), p. 229.
[3] J. B. Parkinson and D. J. J. Farnell, in *An Introduction to Quantum Spin Systems*, Lecture Notes in Physics (Springer-Verlag, Berlin, 2010), Chap. 11.
[4] A. W. Sandvik, Phys. Rev. B **56**, 11678 (1997).
[5] C. J. Hamer, Zheng Weihong, and P. Arndt, Phys. Rev. B **46**, 6276 (1992).
[6] Zheng Weihong, J. Oitmaa, and C. J. Hamer, Phys. Rev. B **43**, 8321 (1991).
[7] E. Manousakis, Rev. Mod. Phys. **63**, 1 (1991).
[8] R. F. Bishop, D. J. J. Farnell, and J. B. Parkinson, Phys. Rev. B **58**, 6394 (1998).
[9] R. F. Bishop, P. H. Y. Li, R. Darradi, J. Schulenburg, and J. Richter, Phys. Rev. B **78**, 054412 (2008).
[10] R. F. Bishop, P. H. Y. Li, R. Darradi, and J. Richter, J. Phys.: Condens. Matter **20**, 255251 (2008).
[11] R. Darradi, J. Richter, J. Schulenburg, R. F. Bishop, and P. H. Y. Li, J. Phys.: Conf. Ser. **145**, 012049 (2009).
[12] R. Darradi, O. Derzhko, R. Zinke, J. Schulenburg, S. E. Krüger, and J. Richter, Phys. Rev. B **78**, 214415 (2008).
[13] J. Oitmaa and Zheng Weihong, Phys. Rev. B **54**, 3022 (1996).
[14] R. R. P. Singh, W. Zheng, C. J. Hamer, and J. Oitmaa, Phys. Rev. B **60**, 7278 (1999).
[15] V. N. Kotov, J. Oitmaa, O. Sushkov, and W. Zheng, Philos. Mag. B **80**, 1483 (2000).
[16] J. Sirker, W. Zheng, O. P. Sushkov, and J. Oitmaa, Phys. Rev. B **73**, 184420 (2006).
[17] T. Pardini and R. R. P. Singh, Phys. Rev. B **79**, 094413 (2009).
[18] E. Dagotto and A. Moreo, Phys. Rev. Lett. **63**, 2148 (1989); Phys. Rev. B **39**, 4744(R) (1989).
[19] H. J. Schulz and T. A. L. Ziman, Europhys. Lett. **18**, 355 (1992); H. J. Schulz, T. A. L. Ziman, and D. Poilblanc, J. Phys. I **6**, 675 (1996).
[20] J. Richter and J. Schulenburg, Eur. Phys. J. B **73**, 117 (2010).
[21] L. Isaev, G. Ortiz, and J. Dukelsky, Phys. Rev. B **79**, 024409 (2009).
[22] B. S. Shastry and B. Sutherland, Physica B **108**, 1069 (1981).
[23] R. Darradi, J. Richter, and D. J. J. Farnell, Phys. Rev. B **72**, 104425 (2005).
[24] D. J. J. Farnell, J. Richter, R. Zinke, and R. F. Bishop, J. Stat. Phys. **135**, 175 (2009).
[25] R. F. Bishop, P. H. Y. Li, D. J. J. Farnell, and C. E. Campbell, Phys. Rev. B **79**, 174405 (2009).
[26] A. Collins, J. McEvoy, D. Robinson, C. J. Hamer, and W. Zheng, Phys. Rev. B **73**, 024407 (2006); **75**, 189902(E) (2007).
[27] A. Collins, J. McEvoy, D. Robinson, C. J. Hamer, and W. Zheng, J. Phys.: Conf. Ser. **42**, 71 (2006).
[28] W. Zheng, J. Oitmaa, and C. J. Hamer, Phys. Rev. B **75**, 184418 (2007); **76**, 189903(E) (2007).
[29] J. Villain, J. Phys. (France) **38**, 385 (1977); J. Villain, R. Bidaux, J. P. Carton, and R. Conte, *ibid.* **41**, 1263 (1980).
[30] R. F. Bishop, Theor. Chim. Acta **80**, 95 (1991).
[31] R. F. Bishop, in *Microscopic Quantum Many-Body Theories and their Applications*, Lecture Notes in Physics Vol. 510, edited by

J. Navarro and A. Polls (Springer-Verlag, Berlin, 1998), p. 1.
[32] D. J. J. Farnell and R. F. Bishop, in *Quantum Magnetism*, Lecture Notes in Physics Vol. 645, edited by U. Schollwöck, J. Richter, D. J. J. Farnell, and R. F. Bishop (Ref. 1), p. 307.
[33] D. J. J. Farnell, R. F. Bishop, and K. A. Gernoth, Phys. Rev. B **63**, 220402(R) (2001).
[34] S. E. Krüger, J. Richter, J. Schulenburg, D. J. J. Farnell, and R. F. Bishop, Phys. Rev. B **61**, 14607 (2000).
[35] D. Schmalfuß, R. Darradi, J. Richter, J. Schulenburg, and D. Ihle, Phys. Rev. Lett. **97**, 157201 (2006).
[36] C. Zeng, D. J. J. Farnell, and R. F. Bishop, J. Stat. Phys. **90**, 327 (1998).
[37] We use the program package "Crystallographic Coupled Cluster Method" (CCCM) of D. J. J. Farnell and J. Schulenburg, see http://www-e.uni-magdeburg.de/jschulen/ccm/index.html
[38] D. J. J. Farnell and R. F. Bishop, Int. J. Mod. Phys. B **22**, 3369 (2008).
[39] P. M. Morse and H. Feshbach, *Methods of Theoretical Physics, Part II* (McGraw-Hill, New York, 1953).
[40] H. Kontani, M. E. Zhitomirsky, and K. Ueda, J. Phys. Soc. Jpn. **65**, 1566 (1996).
[41] W. Marshall, Proc. R. Soc. London, Ser. A **232**, 48 (1955).
[42] J. Igarashi, J. Phys. Soc. Jpn. **62**, 4449 (1993).
[43] K. J. Runge, Phys. Rev. B **45**, 7229 (1992); **45**, 12292 (1992).
[44] H. X. He, C. J. Hamer, and J. Oitmaa, J. Phys. A **23**, 1775 (1990).
[45] M. P. Gelfand, R. R. P. Singh, and D. A. Huse, J. Stat. Phys. **59**, 1093 (1990).
[46] M. P. Gelfand, Solid State Commun. **98**, 11 (1996).
[47] Zheng Weihong, R. H. McKenzie, and R. P. Singh, Phys. Rev. B **59**, 14367 (1999).
[48] T. Pardini and R. R. P. Singh, Phys. Rev. B **77**, 214433 (2008).